SOLID STATE CHEMISTRY

Annual Research Highlights

(1) $(TiO_2)_{1-x}(TaON)_x$ Solid Solution for Band Engineering of Anatase TiO_2

Band engineering of anatase TiO_2 was achieved by means of an anatase $(TiO_2)_{1-x}(TaON)_x$ (TTON) solid solution. Epitaxial thin films of TTON ($0.1 \leq x \leq 0.9$) were synthesized by nitrogen plasma-assisted pulsed laser deposition. Epitaxial growth of anatase TTON was confirmed by X-ray diffraction. The lattice constants of the TTON thin films increased with TaON content in accordance with Vegard's law, indicating formation of a complete solid solution. The bandgaps, band alignment, and refractive indices of the TTON thin films were investigated by combination of spectroscopic ellipsometry and X-ray photoelectron spectroscopy. The bandgap of the anatase TTON systematically decreased with increasing *x*, mainly because of an upward shift in the valence band maximum caused by broadening of the valence band as a result of hybridization of the shallow N 2p orbital. The position of the conduction band minimum was rather insensitive to chemical composition, which makes the band alignment of anatase TTON suitable for photocatalytic water splitting with visible light (Fig. 1c). The refractive index of anatase TTON monotonically increased with an increase in *x* (Fig. 1a,b).

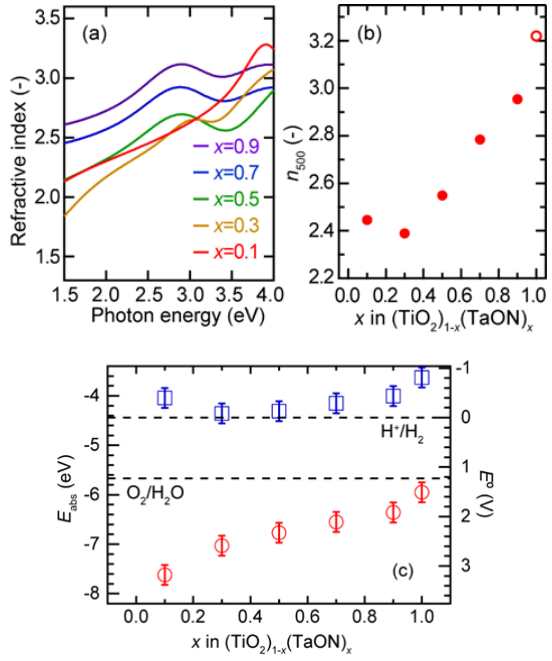

Fig. 1 (a) Refractive index spectra of the anatase TTON thin films. (b) Refractive index at λ = 500 nm (n_{500}) plotted against *x*. (c) Band alignment plotted against the energy of vacuum level (left axis) and the standard electrode potential at 298 K (right axis). Error bars represent the uncertainty in the E_{abs} of O 1s (±0.2 eV) which is used as a reference. Dashed lines represent the $E°(H^+/H_2)$ and $E°(O_2/H_2O)$.

1.(1)-3) *Chem. Mater.*, **30**, 8789 (2018)

(2) Synthesis and magnetism of double-perovskite $YBaCo_2O_6$ thin films

A-site cation-ordered perovskite cobaltite, $RBaCo_2O_x$ (*R* = rare earth element), exhibits fascinating physical properties, such as spin-state ordering and high oxygen conductivity, because of the large tetragonal distortion of the Co orbital. However, the distorted coordination geometry prefers oxygen vacancies, resulting in a difficulty in obtaining the stoichiometric phase ($x = 6$). For example, *x* in $YBaCo_2O_x$, which has largely distorted Co orbitals because of the small size of Y^{3+}, has so far been limited to 5.52. To expand the available range of *x*, in this study, we performed a low-temperature topotactic oxidation of $YBaCo_2O_{5.3}$ epitaxial films using a strong oxidizing agent NaClO. The *x* value can be varied in a wide range of 5.3 – 6.0, maintaining the A-site cation-ordered perovskite structure, by changing the pH and temperature of NaClO. The single crystalline film with $x = 6$ exhibits large tetragonal distortion (c/a = 0.968) because of the small ionic radius of Y^{3+} and substrate-induced tensile strain. Unlike antiferromagnetic insulating $YBaCo_2O_{5.5}$, the fully oxidized film with x = 6 exhibits in-plane ferromagnetism and metallicity with a Curie temperature of 130 K possibly because of the double-exchange interaction between Co^{3+} and Co^{4+} (Fig. 2). Moreover, the $YBaCo_2O_6$ film exhibits huge magnetic anisotropy with a magnetic anisotropy constant of 1.5×10^8 erg cm^{-3}, demonstrating that the A-site cation-ordered perovskite structure is promising for obtaining high magnetocrystalline anisotropic materials.

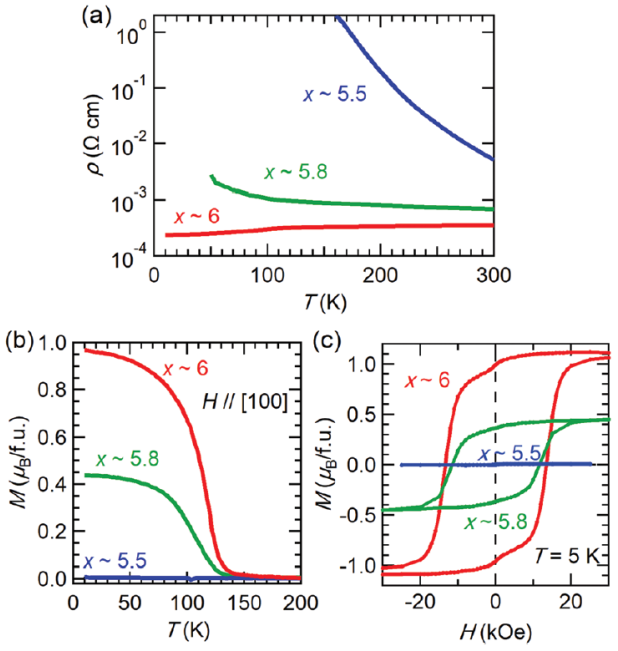

Fig. 2 (a) ρ–*T*, (b) *M*–*T*, and (c) *M*–*H* curves for the $YBaCo_2O_x$ films with $x = 5.5$, 5.8, and 6.0.

2.(1)-17) *J. Mater. Chem. C*, **6**, 3445 (2018).

固体化学研究室

余白
上下:25–30mm
左右:20–25mm

研究ハイライト

(1) アナターゼ TiO_2 と TaON の固溶体によるバンドエンジニアリング

光触媒や透明導電膜、薄膜トランジスタなどに応用されている代表的な酸化物半導体であるアナターゼ TiO_2 にアナターゼ型酸窒化物 TaON を固溶することで、バンドエンジニアリングと光学特性の制御を実現した。窒素プラズマ支援パルスレーザー堆積法で LSAT 基板上にエピタキシャル成長したアナターゼ$(TiO_2)_{1-x}(TaON)_x$固溶体(TTON)薄膜は、全組成域において格子定数が線形に変化する全率固溶系であった。X 線光電子分光と分光エリプソメトリーによりバンド端のポテンシャルを評価したところ、浅い N 2p 軌道の影響により TaON 量 x が増えるにつれて価電子帯上端が単調に上側にシフトした。一方、伝導帯下端の位置はほとんど変化しなかった。結果として、TTON は水の全分解光触媒反応に適したバンドアライメントを保ちつつ、可視光応答性を示すことが明らかになった（図 1c)。また、共有結合性の高い N の効果により、x の増大に伴って屈折率は単調に増大した（図 1a,b)。

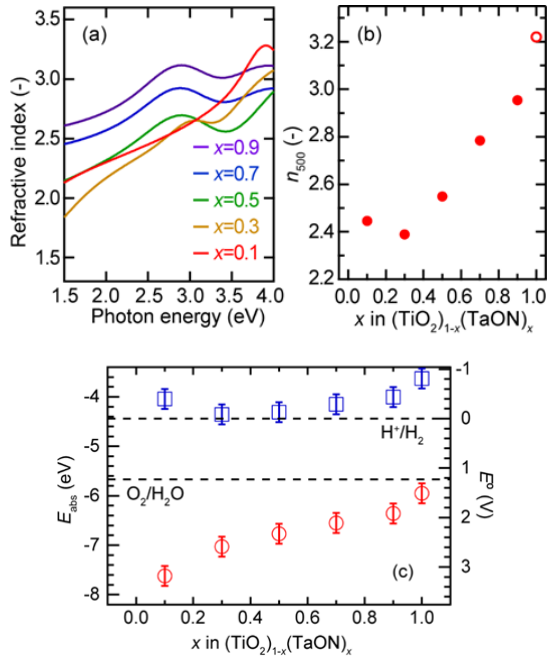

図 1 LSAT 基板上に合成したアナターゼ$(TiO_2)_{1-x}(TaON)_x$エピタキシャル薄膜の(a)屈折率スペクトル、(b)波長 500nm における屈折率、および(c)バンドアライメントと組成 x の関係。(c)の左軸は真空準位を基準としたポテンシャル、右軸は標準電極電位。破線は $E°(H^+/H_2)$ と $E°(O_2/H_2O)$を示す。

1.(1)-3) *Chem. Mater.*, **30**, 8789 (2018)

(2) ダブルペロブスカイト $YBaCo_2O_6$ エピタキシャル薄膜の合成と磁性

A サイト秩序ダブルペロブスカイト構造を有する $RBaCo_2O_x$（*R* は希土類元素）はスピン状態秩序、高酸素伝導など様々な興味深い物性を示す。しかし、Co 軌道が大きく歪んでいるため酸素欠損が生じやすく、酸素が埋まった $x = 6$ の試料を得ることは難しい。例えば、$YBaCo_2O_x$ の x の値はこれまで 5.52 以下に限られていた。本研究では $YBaCo_2O_x$ の酸素量を大幅に増やすため、強酸化剤である NaClO を用いた低温トポタクティック反応を試みた。その結果、ダブルペロブスカイト構造を保ったまま x の値を 5.3-6.0 の幅広い範囲で制御することに成功した。また酸素量制御において pH や温度の調整が重要であることを見出した。得られた $YBaCo_2O_6$ 膜はキュリー温度 130 K の強磁性であり金属伝導を示した。これは絶縁体で反強磁性の $YBaCo_2O_{5.5}$ 膜とは異なる挙動である（図 2)。さらに $YBaCo_2O_6$ 膜は面内に大きな磁気異方性を示した。これは結晶構造由来の歪み(c/a = 0.968)に由来する。

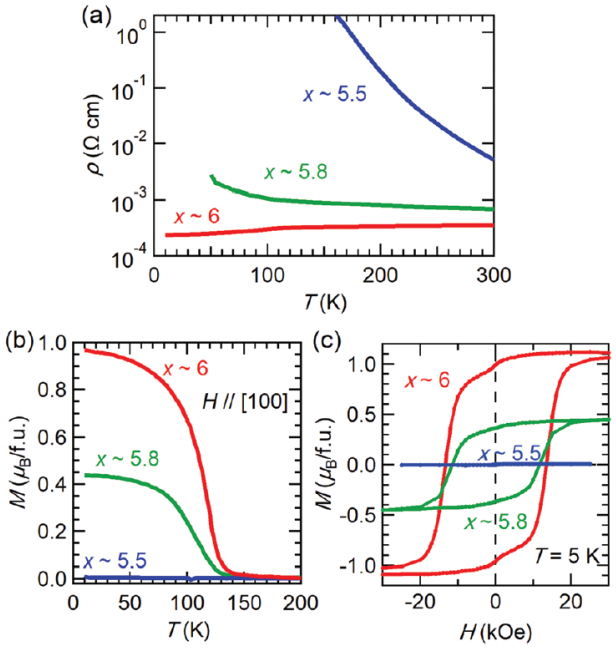

図 2 酸素量の異なる $YBaCo_2O_x$ 薄膜（x = 5.5、5.8、6.0）の(a)抵抗率の温度依存性、(b)磁化の温度依存性、(c)磁化の磁場依存性。

2.(1)-17) *J. Mater. Chem. C*, **6**, 3445 (2018).

1. 原著論文

(1) Refereed Journals

1) D. Kutsuzawa, Y. Hirose, A. Chikamatsu, S. Nakao, Y. Watahiki, I. Harayama, D. Sekiba, and T. Hasegawa, "Strain-enhanced topotactic hydrogen substitution for oxygen in $SrTiO_3$ epitaxial thin film", *Appl. Phys. Lett.* **113**, 253104 (2018).
2) T. Toyoda, Q. Shen, M. Hironaka, K. Kamiyama, H. Kobayashi, Y. Hirose, and S. Hayase, "Anisotropic Crystal Growth, Optical Absorption, and Ground-State Energy Level of CdSe Quantum Dots Adsorbed on the (001) and (102) Surfaces of Anatase-TiO_2: Quantum Dot-Sensitization System", *J. Phys. Chem. C*, **122**, 29200 (2018).
3) A. Suzuki, Y. Hirose, S. Nakao, and T. Hasegawa, "$(TiO_2)_{1-x}(TaON)_x$ Solid Solution for Band Engineering of Anatase TiO_2", *Chem. Mater.*, **30**, 8789 (2018).
4) K. Terakado, R. Sei, H. Kawasoko, T. Koretsune, D. Oka, T. Hasegawa, and T. Fukumura, "Superconductivity in Anti-$ThCr_2Si_2$-type Er_2O_2Bi Induced by Incorporation of Excess Oxygen with CaO Oxidant", *Inorg. Chem.*, **57**, 10587 (2018).
5) M. Okuya, J. Sato, T. Endo, R. Iwaki, S. Takemura, R. Muramoto, V. Nagygyőrgy, J. Madarász, S. Nakao, N. Yamada, E. Sakai, T. Hitosugi, and T. Hasegawa, "TiO_2/TNO homojunction introduced in a dye-sensitized solar cell with a novel TNO transparent conductive oxide film", *J. Am. Ceram. Soc.* **101**, 5071 (2018).
6) A. Chikamatsu, K. Kawahara, T. Shiina, T. Onozuka, T. Katayama, and T. Hasegawa, "Fabrication of Fluorite-Type Fluoride $Ba_{0.5}Bi_{0.5}F_{2.5}$ Thin Films by Fluorination of Perovskite $BaBiO_3$ Precursors with Poly(vinylidene fluoride)", *ACS Omega*, **3**, 13141 (2018).
7) C. Yang, Y. Hirose, T. Wakasugi, N. Kashiwa, H. Kawai, K. Yamashita, and T. Hasegawa, "Epitaxial Growth of $(GaN)_{1-x}(ZnO)_x$ Thin Films with Wide Chemical Composition Tunability and Strong Visible Absorption", Phys. Rev. Appl., **10**, 044001 (2018).
8) K. Kaminaga, D. Oka, T. Hasegawa, and T. Fukumura, "New Lutetium Oxide: Electrically Conducting Rock-Salt LuO Epitaxial Thin Film", *ACS Omega*, **3**, 12501 (2018).
9) D. Oka, Y. Hirose, M. Kaneko, S. Nakao, T. Fukumura, K. Yamashita, and T. Hasegawa, "Anion-Substitution-Induced Non-Rigid Variation of Band Structure in $SrNbO_{3-x}N_x$ ($0 \leq x \leq 1$) Epitaxial Thin Films", *ACS Appl. Mater. Interfaces*, **10**, 35008 (2018).
10) T. Onozuka, A. Chikamatsu, Y. Hirose, and T. Hasegawa, "Structural and electrical properties of lanthanum copper oxide epitaxial thin films with different domain morphologies", *CrystEngComm*, **20**, 5012 (2018).
11) A. Suzuki, Y. Hirose, T. Nakagawa, S. Fujiwara, S. Nakao, Y. Matsuo, I. Harayama, D. Sekiba, and T. Hasegawa, "Enhanced Electrical Conduction in Anatase TaON via Soft Chemical Lithium Insertion toward Electronics Application", ACS Appl. Nano Mater., **1**, 3981 (2018).
12) M. Oka, H. Kamisaka, T. Fukumura, and T. Hasegawa, "Density functional theory-based *ab initio* molecular dynamics simulation of ionic conduction in N-/F-doped ZrO_2 under epitaxial strain", *Comp. Mater. Sci.* **154**, 91 (2018).
13) T. Maruyama, A. Chikamatsu, T. Onozuka, and T. Hasegawa, "Magnetotransport properties of perovskite $EuNbO_3$ single-crystalline thin films", *Appl. Phys. Lett.* **113**, 032401 (2018).
14) A. Chikamatsu, Y. Kurauchi, K. Kawahara, T. Onozuka, M. Minohara, H. Kumigashira, E. Ikenaga, and T. Hasegawa, "Spectroscopic and theoretical investigation of the electronic states of layered perovskite oxyfluoride $Sr_2RuO_3F_2$ thin films", *Phys. Rev. B* **97**, 235101-1-7 (2018).
15) K. Kaminaga, D. Oka, T. Hasegawa, and T. Fukumura, "Superconductivity of Rock-Salt Structure LaO Epitaxial Thin Film", *J. Am. Chem. Soc.*, **140**, 6754 (2018).
16) M. Fukumoto, S. Nakao, Y. Hirose, and T. Hasegawa, "Fabrication of textured SnO_2 transparent conductive films using self-assembled Sn nanospheres", *Jpn. J. Appl. Phys.* **57**, 060307 (2018).
17) T. Katayama, A. Chikamatsu, Y. Hirose, M. Minohara, H. Kumigashira, I. Harayama, D. Sekiba, and T. Hasegawa, "Ferromagnetism with strong magnetocrystalline anisotropy in A-site ordered perovskite $YBaCo_2O_6$ epitaxial thin film prepared via wet-chemical topotactic oxidation", *J. Mater. Chem. C* **6**, 3445 (2018).
18) V. Motaneeyachart, Y. Hirose, A. Suzuki, S. Nakao, I. Harayama, D. Sekiba, and T. Hasegawa, "Epitaxial Growth of Baddeleyite NbON Thin Films on Yttria-Stabilized Zirconia by Pulsed Laser Deposition", *Chem. Lett.* **47**, 65 (2018).

19) S. Shibata, R. Sei, Tomoteru Fukumura, and Tetsuya Hasegawa, “Magnetic and magnetotransport properties of $ThCr_2Si_2$-type Ce_2O_2Bi composed of conducting Bi^{2-} square net and magnetic Ce–O layer”, *Appl. Phys. Lett.* **110**, 192410 (2018).

(2) その他

2. 総説・解説

3. 著書

4. その他